Description of numerical shock profiles of non-linear Burgers' equation by asymptotic solution of its differential approximations

A. V. Porubov, D Bouche, G Bonnaud

Description of numerical shock profiles of non-linear Burgers' equation by asymptotic solution of its differential approximations

A.V. Porubov[1]

[1] *Institute for Problems in Mechanical Engineering, Bolshoy 61, V.O., Saint-Petersburg 199178, Russia*

porubov@math.ioffe.ru

D. Bouche[2,3]

[2] *CMLA, ENS de Cachan, Cachan, France*

[3] *CEA, DIF/DPTA, BP12, 91680, Bruyères le Châtel, France*

daniel.bouche@cea.fr

G.Bonnaud[4]

[4] *CEA, INSTN, Centre de Saclay, 91191, Gif-sur-Yvette, France*

guy.bonnaud@cea.fr

Abstract

An analysis of dispersive/dissipative features of the difference schemes used for simulations of the non-linear Burgers' equation is developed based on the travelling wave asymptotic solutions of its differential approximation. It is shown that these particular solutions describe well deviations in the shock profile even outside the formal applicability of the asymptotic expansions, namely for shocks of moderate amplitudes. Analytical predictions may be used to improve calculations by suitable choice of the parameters of some familiar schemes, i.e., the Lax-Wendroff, Mac-Cormack etc. Moreover, an improvement of the scheme may be developed by adding artificial terms according to the asymptotic solution.

Key words : Scheme dispersion and dissipation, non-linear shock wave, asymptotic and numerical solutions.

1 Motivation of the work

Numerical solutions by finite volume or finite difference schemes of fast-changing processes or problems containing discontinuities may produce non-physical perturbations of the shape of the solution. More specifically, numerical shock profiles often exhibit either oscillations or excessive smearing, as compared with exact solutions. The theory of differential equations is employed to account for these defects of numerical schemes using the method of differential approximation [Sh 83]. A differential approximation is obtained using a substitution of the Taylor expansions of the discrete functions into a difference scheme. An analysis of the resulting partial differential equation (PDE) is possible if the expansion is truncated at some order. The PDE is called the first differential approximation if only terms of order of the scheme approximation are taken into account. It turns out that, for the linear advection equation, the first differential approximation predicts in the bulk the behaviour of the scheme. However, the method of differential approximation with more terms provides more accurate prediction of the behaviour of the scheme [BBR 03, MPP83]. In particular, the differential approximation for the linear advection equation

$$u_t + u_x \ = \ 0$$

designed by a numerical scheme (either finite difference or finite volumes) is written as [Sh 83, BBR 03, MPP83]

$$u_t + u_x \ = \ \ - b\ u_{xx} - s\ u_{xxx} - q\ u_{xxxx}, \tag{1}$$

where b, s, q depend upon the parameters of the scheme used. An influence of the scheme dispersion is accounted for the second term in the r.h.s. of Eq.(1), while the first and the third ones are responsible for dissipation. Solutions of Eq.(1) allow us to explain and reproduce oscillations of numerical shock profiles of second and third (b = 0 in this case) order schemes [BBR 03, MPP83].

The analysis becomes more complicated when the non-linear advection equation,

$$u_t + u\ u_x \ = 0 \tag{2}$$

is considered. In this case, a differential approximation for a second order scheme is [Sh 83, LP 75, E 99]

$$u_t + u\ u_x = -b(u)\ u_{xx} - s(u)\ u_{xxx} + \alpha(u, u_x) - q(u)\ u_{xxxx}, \tag{3}$$

Specific schemes, like the Lax-Wendroff, Mac-Cormack, Warming-Beam etc. may be expressed in this form as will be shown in the paper. The first three terms on the r.h.s. stem from the first differential approximation of the scheme. The fourth appears among others when second differential approximation of second order schemes or first differential approximation of third order scheme is considered. Previously, the importance of the fourth order dissipation for accurate prediction of numerical shock profile has been demonstrated for the linear advection equation [BBR 03]. Now b, s, q depend also on u, and α depends upon its arguments non-linearly. Hence, the r.h.s. of Eq.(3) is nonlinear in u and u_x, that makes probably

impossible finding exact solutions. That is why it was suggested in [MPP 83] to consider weakly nonlinear case around some constant value of u linearizing only the r.h.s. of Eq.(3). In particular, the Korteweg-de-Vries equation follows from Eq.(3) for $b = 0,\ q = 0,\ s = const, \alpha = 0$, while the Burgers equation is obtained for $b = const,\ s = 0,\ q = 0,\ \alpha = 0$. Known analytical solutions of these *integrable* equations [AS 81, W 74] allowed authors of Ref. [MPP 83] to describe dissipative and dispersive properties of the schemes they used. To predict more accurately the shapes of numerical shock profiles, it will be useful to obtain the travelling wave solution of the above equation. However, Eq.(3) is *non- integrable* either in the presence of arbitrary two constant nonzero coefficients b, s, q, or in the general non-linear case, $b = b(u)$, $s = s(u)$, $q = q(u), \alpha \neq 0$. Then, even obtaining a particular exact travelling wave solutions existing at specific initial conditions is not guaranteed. Moreover, only particular asymptotic solutions may be found. Then a natural question arises: may particular solutions be used to analyze the features of the differential approximations, thus the features of the difference schemes? There is no universal answer for non-integrable equations, and our consideration now is restricted to rather simple non-linear advection equation with viscosity, namely the Burgers' equation, in order to present our main ideas in a form convenient for readers excluding huge analytical formuli.

In this paper, we demonstrate the efficiency of the use of particular asymptotic travelling waves solutions of Eq.(3) for understanding the deviations in the shock caused by the scheme features. It is shown, that unsteady numerical solutions obtained using the Lax-Wendroff, Warming-Beam and some other schemes approach the shape predicted by the asymptotic solution of the differential approximation and even for moderate values of the shock amplitude, thus outside the formal applicability of the solution. A possibility is studied to suppress deviations caused by a scheme dispersion by adding artificial non-linear terms predicted by an asymptotic solution of the differential approximation.

2 Propagation of the shocks governed by the differential approximation

Let us consider Eq. (3) as a perturbed non-linear Burgers equation. In the case when a scheme with only dispersive features is used, an artificial viscosity, $b\ u_{xx}$, is included into Eq. (3) [MPP 83, LP 75].

In the case $b(u) = b, s = \alpha = q = 0$ the differential approximation (3) is the non-linear Burgers equation,

$$L(u) = u_t + u\ u_x + b\ u_{xx} = 0, \tag{4}$$

and the shock wave may be analyzed by using the exact shock-wave solution (or a kink), see, e.g., [W 74],

$$u_0 = 2\ b\ p\ \tanh(p(X - Vt)) + V. \tag{5}$$

where p and V are free parameters to be defined by the boundary conditions for x,

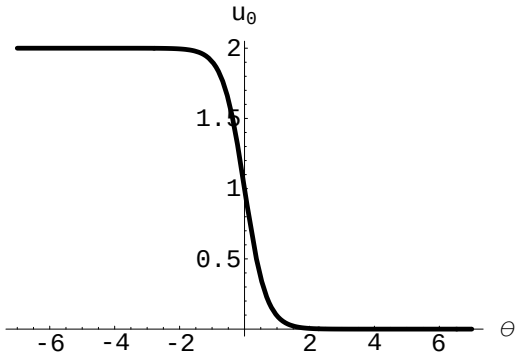

Figure 1: Typical shape of the exact solution of the Burgers equation

i.e., for given values of u at infinities we have

$$V \;=\; (u_\infty + u_{-\infty})/2,\; p \;=\; (u_\infty - u_{-\infty})/(4b).$$

The typical shape of the Burgers exact solution (5) is shown in Fig.1 for $b \,<\, 0, V \,>\, 0$ that demonstrates a smooth monotonic transition from one stable state to another one. This happens because the shock wave of the Burgers equation arises as a result of a balance between nonlinearity and dissipation described by the second and the third terms in Eq.(4) respectively. For the integrable Burgers equation, it is possible to study analytically the elevation for an arbitrary initial condition. However, addition of dispersive and higher-order dissipative terms in the r.h.s of Eq.(4) destroys integrability, and only particular asymptotic solutions may be used for an analysis in the following.

2.1 Influence of weak dispersion

When a scheme possesses dispersion, the simplest description of it in the differential approximation Eq. (3) reads as

$$L(u) = -\delta s\; u_{xxx}, \tag{6}$$

where δ is a small parameter, $s \;=\; const$. Equation (6) is often called the Korteweg de Vries - Burgers equation. Its asymptotic solution is sought in the form

$$u(\theta) = u_0(\theta) + \delta u_1(\theta) + ... \tag{7}$$

where $\theta = x - Vt$, and $u_1 \to 0$ at $\theta \to \pm\infty$. Substituting this series into Eq.(6) we obtain an ordinary differential equation (ODE) in the leading order,

$$(-V\; u_0 + 0.5u_0^2 + b\; u_{0,\theta})_\theta \;=\; 0,$$

which is satisfied by the solution (5). In the next order an inhomogeneous linear ODE appears for the function u_1,

$$(-V\; u_1 +\; u_0 u_1 + b\; u_{1,\theta})_\theta \;=\; -\,s\; u_{0,\theta\theta\theta},$$

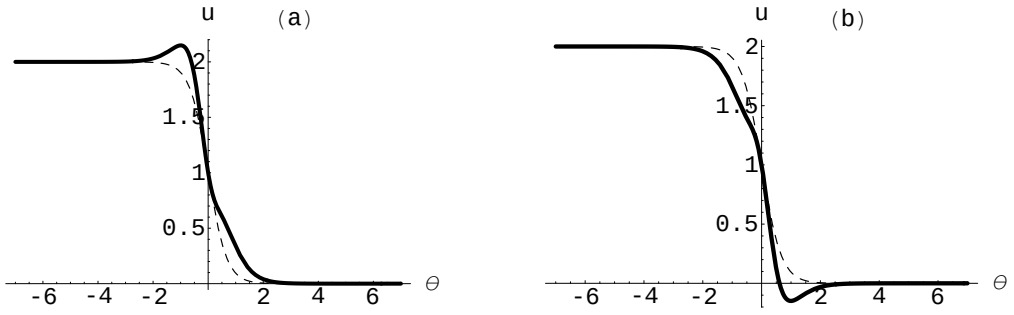

Figure 2: Influence of the weak dispersion on the Burgers shock wave solution: a) $s > 0$; b) $s < 0$.

whose solution is

$$u_1 = 4\ p^2 s \cosh(p\theta)^{-2} \log(\cosh(p\ \theta)) \tag{8}$$

Figure 2 demonstrates the influence of the weak dispersion on the shape of the Burgers shock wave. Here and in the following the unperturbed solution is shown by dashed line while the first two terms in the expansion, $u = u_0 + \delta u_1$, are shown by solid line. One can note non-symmetric influence on the upper and lower parts of the shock. At positive s, Fig. 2(a), a "hat" appears at the upper part of the shock while the lower one exhibits a smoother profile. The mirror profile appears at negative values of s, Fig.2(b). We see that all deviations are concentrated around the wave front. All these features may be studied analytically using the standard analysis of the first derivative of u.

Similar deviations in the wave profile were also obtained in numerical study of the non-linear advection equation [MPP 83, LP 75]. It should be noted that the approach used in [MPP 83] usually provides a condition required for oscillations, while our solution allows us to describe the shape of the wave and to predict where oscillations appear, on the lower or on the upper part of the shock.

2.2 Influence of weak higher-order dissipation

Let us consider the case when dispersion is absent, $s = 0, \alpha = 0$, and higher-order dissipation is weak, and Eq. (3) is written as

$$L(u) = -\delta q\ u_{xxxx}, \tag{9}$$

where q is a constant. In particular the above equation appears as a simplified version of the differential approximation of the discretization of the non linear advection equation by a third-order scheme[E 99].

Now the addition to the leading order solution u_0 is

$$u_1 = \frac{4p\ q}{b}\ u_{0,\theta}\,(3\tanh(p\theta) - 2p\ \theta) \tag{10}$$

We see in Fig.3 that the solution $u = u_0 + \delta u_1$ describes now symmetric deviations in the shock wave profile which is clearly seen from its first derivative.

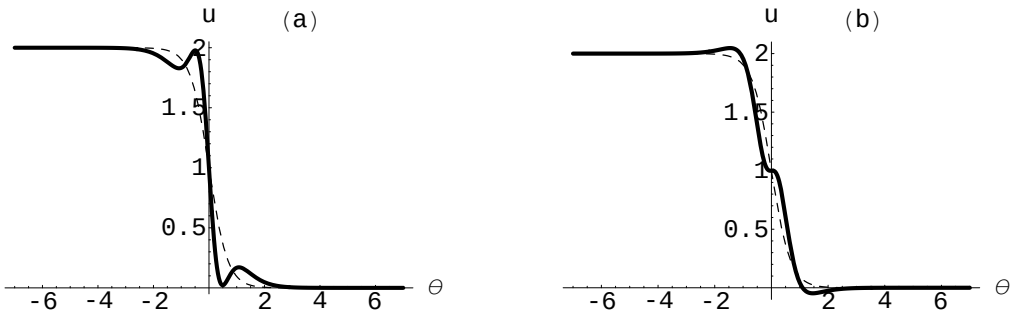

Figure 3: Influence of the higher-order dissipation on the Burgers shock wave solution: a) $q < 0$; b) $q > 0$.

However, they are different for positive and negative values of q. At negative q in Fig.3(a) both the upper and the lower parts are perturbed so the small cavities appear. The additional maxima (or "hats") appear for positive q in Fig.3(b). This differs from the previous case when a "hat" appears for either sign of the dispersion coefficient but only at one side of the shock.

2.3 Influence of nonlinear perturbations

It is also possible to obtain asymptotic solutions for non- linear r.h.s in Eq.(3). Indeed, let us consider the case

$$L(u) = -\delta\alpha(u^3)_{xx}, \tag{11}$$

where α is a constant. It happens for $b(u) = b+3\delta\ \alpha\ u^2$, $s(u) = 0$, $\alpha(u, u_x) = -6\delta\ \alpha\ uu_x^2$, $q(u) = 0$. Also, the case $\alpha > 0$ in Eq. (11) corresponds to the differential approximation arising for the first-order scheme mentioned on page 265 in Shokin's book [Sh 83]. The addition to the leading order solution u_0 has the form

$$u_1 = 6\ b\ p^2\ \alpha\ \cosh(p\ \theta)^{-2}\left(\ b\ p\ \tanh(p\ \theta) - (bp^2 + \frac{V^2}{4b})\theta - \ V\ \log[\cosh(p\ \theta)]\right) \tag{12}$$

The perturbations of the shock wave is shown in Fig.4 for different signs of α. A "hat" arising at positive values of α at Fig.4(a) looks similar to that arising in the weakly dispersive case, at Fig. 3(a) for $s > 0$. However, deviations of the upper part of the solution shown in Fig.4(b) are opposite to those arising in the weakly dispersive case for $s > 0$ by additional influence. Since the influence of perturbations is described by means of a linear ODE, the superposition principle is valid. Thus, perturbation u_1 for the equation below, combining dispersion and cubic non-linearity is the superposition of perturbations computed above. Let us assume that u satisfies

$$L(u) = -\delta(s\ u_{xxx} + \alpha(u^3)_{xx}), \tag{13}$$

Using above found asymptotic solutions one can select the values of the coefficients α and s so as to compensate the hat produced by dispersion, and to get an asymptotic

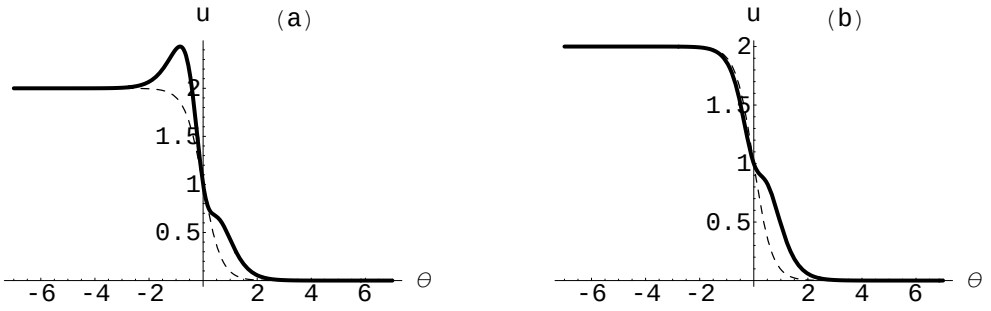

Figure 4: Influence of the higher-order cubic nonlinearity on the Burgers shock wave: a) $\alpha > 0$; b) $\alpha < 0$.

solution describing propagation of the smooth shock without "hat". This observation allows us to suggest possible improvement of the schemes by adding artificial nonlinear terms in the difference equation.

3 Evidence of asymptotic behavior in numerical simulations

The solutions obtained in previous section require specific initial condition. However, they predict well deviations in the shock profile caused by a scheme even outside their formal validity. It will be illustrated by analysis of numerical solutions of the nonlinear advection equation (2) using some familiar schemes.

3.1 Second-order schemes

The first scheme we employ is the well-known Lax-Wendroff (LW) second order scheme to the Burgers' equation, whose first differential approximation reads

$$u_t + u\ u_x\ + bu_{xx} = \frac{\triangle t^2}{24}(u^4)_{xxx}\ -\ \frac{\triangle x^2}{12}(u^2)_{xxx}, \tag{14}$$

that corresponds to Eq.(3). Being linearized around boundary value $u_{-\infty}$, the r.h.s. of Eq.(14) gives rise to the r.h.s. of Eq.(6) with

$$\delta s\ =\ \frac{\left(\triangle x^2 - \triangle t^2 u_{-\infty}^2\right) u_{-\infty}}{6}, \tag{15}$$

The positive sign of the dispersion coefficient s cannot be changed without exceeding the stability criterium $u_{-\infty}\triangle t\ <\ \triangle x$. According to the asymptotic solution obtained in Sect. 2.1 an upper part of the shock should be disturbed, and these disturbances will be weaker for higher temporal step since s decreases with increase in $\triangle t$. The following values for the steps are used in computations, $\triangle x\ =\ 1$, $\triangle t\ =\ 0.2$ and $\triangle t\ =\ 0.5$. The moderate value of $u_{-\infty} - u_{\infty}\ =\ 2$ is chosen outside a formal applicability of the linearization of Eq.(3), $|u - u_{-\infty}| << 1$. The value

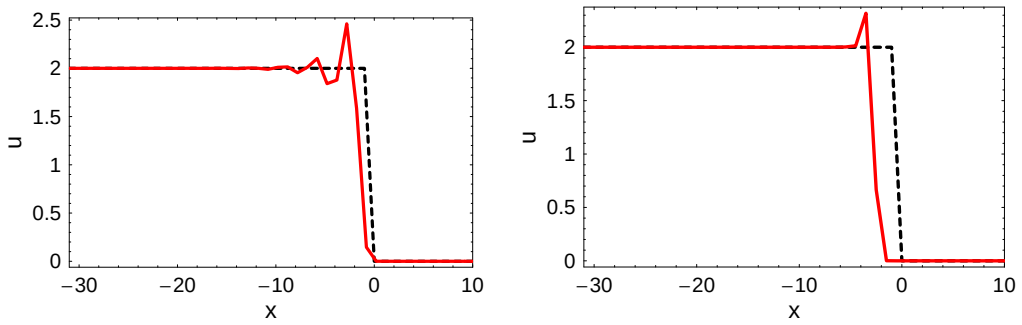

Figure 5: Propagation of an initial abrupt front using the LW scheme with artificial viscosity at time t = 500 (i.e. the front has propagated along 500 mesh sizes). a) $\triangle t = 0.2$; b)$\triangle t = 0.5$

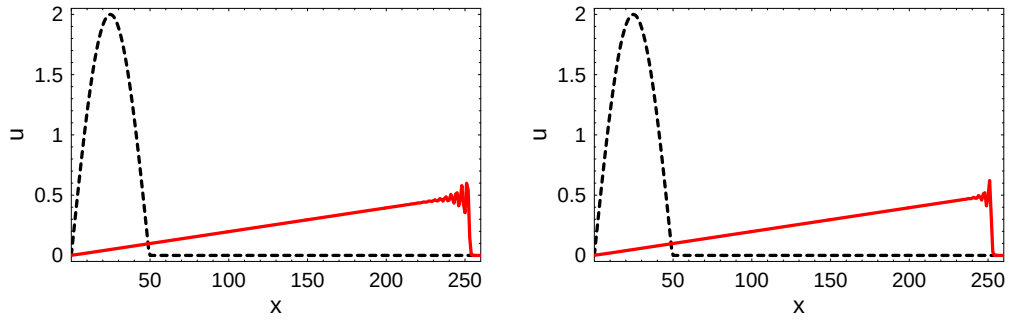

Figure 6: Propagation of an initial localized pulse using the LW scheme with artificial viscosity at time t = 500 (i.e. the front has propagated along 500 mesh sizes). a) $\triangle t = 0.2$; b)$\triangle t = 0.5$

of the coefficient at viscous term is chosen to be small, $b = -0.01$. The initial conditions are used in the form of abrupt front and in the form of the localized pulse. However, in both cases we obtain perturbations in agreement with the asymptotic solution (7),(5), (8) with δs defined by Eq.(15)). Indeed, the position of the overshoot on the upper part of the shock is predicted correctly, c.f. Figs. 5(a), 6(a) and Fig. 2(a). In both figures 5 and 6 the initial abrupt front is shown by dotted line to compare with the profile obtained numerically. Also a decrease in disturbances is observed for higher temporal step, see Figs. 5(b), 6(b). More clearly it is seen in Fig. 7 where the dependence of the values of the height of the overshoot vs temporal step is shown. One can see that the amplitude of the overshoot oscillates within an interval bounded by solid and dotted lines. The oscillation period is exactly the time required for the front to hop from a mesh node to another : for dt = 0.2, the period is observed to be 1 = 5 dt. For dt = 0.4, this period is 2, i.e. 5 dt as well. However, the maximum decreases as the temporal step increases. This is also related to the asymptotic solution since dispersion coefficient s becomes lower as temporal step increases while contribution of the perturbation (8) is proportional to s.

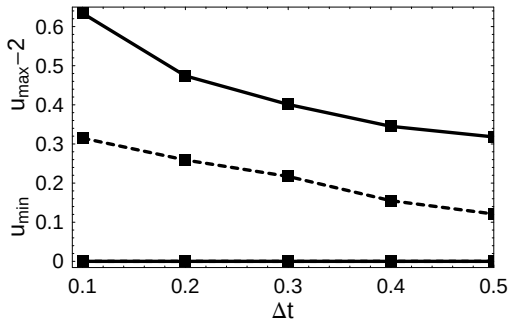

Figure 7: Variations of minimum and maximum of the shock vs temporal step for the LW scheme: $u_{max} - 2$ varies between upper solid line and dotted line, while lower solid line corresponds to u_{min}.

Now we turn to the Warming-Beam (WB) second order scheme [F 91] with artificial viscosity, whose first differential approximation reads

$$u_t + u\ u_x\ + b\ u_{xx} = \frac{\triangle t^2}{24}(u^4)_{xxx}\ -\ \frac{\triangle t\ \triangle x}{6}(u^3)_{xxx} + \frac{\triangle x^2}{6}(u^2)_{xxx}, \tag{16}$$

Being linearized around average value of $u_{-\infty}$, the r.h.s. of Eq.(16) gives rise to the r.h.s. of Eq.(6) with

$$\delta s\ =\ -\frac{u_{-\infty}}{6}\left(\triangle t^2 u_{-\infty}^2 - 3\triangle t\triangle x u_{-\infty} + 2\triangle x^2\right), \tag{17}$$

Analysis of the expression in brackets within the stability criterium domain, $u_{-\infty}\triangle t\ <\ \triangle x$, gives rise to $s\ <\ 0$, and the scheme exhibits negative dispersion. According to the asymptotic solution (7),(5), (8) with δs defined by (17) an undershoot should appear at the lower part of the shock, see Fig.2(b), and numerical results shown in Fig. 8 demonstrate validness of this prediction of the asymptotic solution, namely, the position of the undershoot. One can note from Eqs.(8), (17)) that the absolute value s decreases as δt increases with fixed δx. Asymptotic solution thus predicts a reduction of the undershoot. This is not clearly seen in the figures 8, however, it is confirmed in close look on undershoot amplitude shown in Fig.9. Now the minimum varies in time, however, the highest absolute value of minimum marked by dotted line in Fig.9 becomes slightly smaller as the temporal step growths.

The Mac-Cormack scheme [F 91] with artificial viscosity exhibits the same features of the solution as the LW scheme. Indeed, its differential approximation reads

$$u_t + u\ u_x\ + b\ u_{xx}\ =\ \frac{\triangle t^2}{24}\left(u_{xxx}^4 - 12u(u_x)^3 - 12u^2u_{xx}\right)\ -\ \frac{\triangle x^2}{12}(u^2)_{xxx} - \frac{\triangle t\triangle x}{4}\left((u_x)^3 + 2uu_xu_{xx}\right), \tag{18}$$

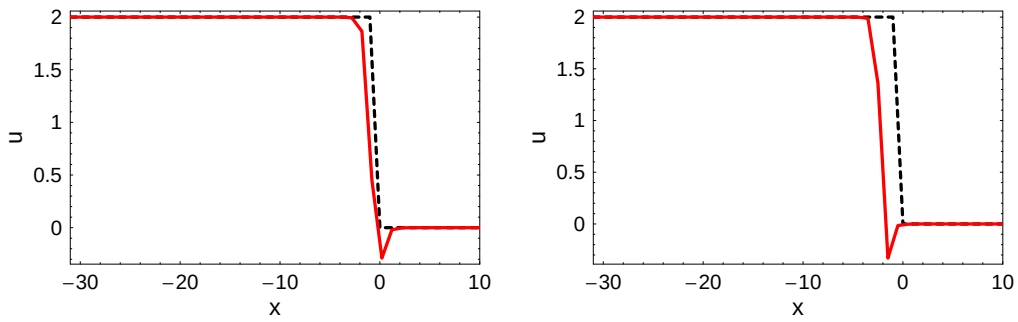

Figure 8: Propagation of an initial abrupt front using the WB scheme with artificial viscosity at time t = 500 (i.e. the front has propagated along 500 mesh sizes). a) $\triangle t = 0.2$; b)$\triangle t = 0.5$.

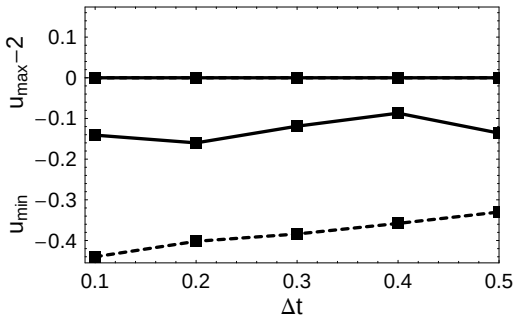

Figure 9: Variations of minimum and maximum of the shock vs temporal step for the WB scheme: upper solid line corresponds u_{max}-2; lower solid line and dotted line- bound values of u_{min}.

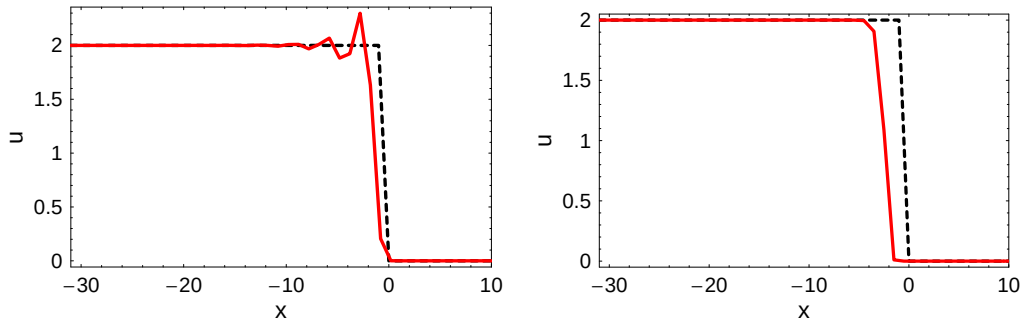

Figure 10: Propagation of an initial abrupt front using the Mac-Cormack scheme with artificial viscosity at time t = 500 (i.e. the front has propagated along 500 mesh sizes). a) $\triangle t = 0.2$; b)$\triangle t = 0.5$.

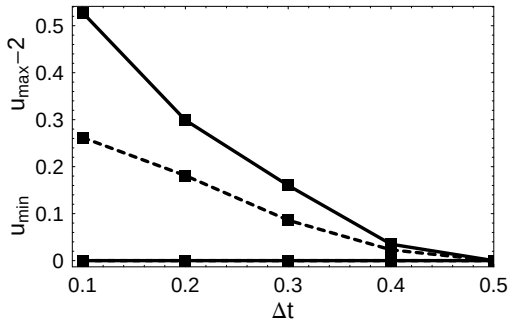

Figure 11: Variations of minimum and maximum of the shock vs temporal step for the MC scheme: u_{max}-2 varies between upper solid line and dotted line while lower solid line corresponds to u_{min}.

Like for the Lax-Wendroff scheme, being linearized around boundary value $u_{-\infty}$, the r.h.s. of Eq.(18) gives rise to the r.h.s. of Eq.(6) with

$$\delta s = \frac{u_{-\infty}}{6}\left(\triangle x^2 - \triangle t^2 u_{\infty}^2\right), \tag{19}$$

Again we have a scheme with positive dispersion, and an agreement about the overshoot position is found comparing Fig. 2(a) and Fig. 10(a). However, almost unperturbed shock profile should be obtained using (19)) for the time period close to the stability criterium since in the last case $s \to 0$ for given $u_{-\infty} = 2$ and $\triangle t = 0.5$. This prediction is confirmed in numerics as follows from Figs. 10(b) and 11.

Figure 11 demonstrates that the high of the overshoot decreases as temporal step growths that analytically follows from Eqs. (8), (19) like for the LW and WB schemes.

3.2 Third-order schemes with weak dissipation

The scheme dispersion may be suppressed by an increase in the order of the consistency error of the LW scheme [BBR 03]. Thus, the third order modification of the Lax-Wendroff scheme (LW3) may be obtained if the terms in the r.h.s. in Eq.(14) are added in the difference scheme for the advection equation with opposite sign according to the upwind discretisation,

$$D_3[g_i^n] \;=\; \frac{-g_{i-2}^n + 3g_{i-1}^n - 3g_i^n + g_{i+1}^n}{\triangle x^3},$$

where $g \;=\; \{u^4,\; u^3\}$. A non-centered upwind scheme is chosen to achieve better stability features. Then instead of Eq.(14) the first differential approximation is obtained of the form,

$$u_t + u\; u_x \;+ b\; u_{xx} \;=$$

$$-\left(\frac{\triangle t^3}{120}(u^5)_{xxxx} \;-\; \frac{\triangle t^2\;\triangle x}{48}(u^4)_{xxxx} + \frac{\triangle t\;\triangle x^2}{72}(9u_x^2u_{xx} - (u^3)_{xxxx}) + \frac{\triangle x^3}{24}(u^2)_{xxxx}\right), \tag{20}$$

This modification gives rise to increase in dissipative properties of the scheme. Indeed, now the linearized l.h.s. of Eq.(20) corresponds to Eq.(9),

$$\delta q \;=\; \frac{u_{-\infty}}{48}\left(2\triangle t^3u_{-\infty}^3 - 3\triangle t^2\;\triangle x u_{-\infty}^2 - 2\triangle t\;\triangle x^2u_{-\infty} + 4\triangle x^3\right), \tag{21}$$

giving positive values of q within the domain of stability. The numerical shock profiles shown in Fig. 12 exhibit symmetric deviations in the shock wave profile, with mirror symmetric hats both on the upper and lower parts of the shock, similar to the asymptotic profile shown in Fig.3 (b) for $q \;>\; 0$. Like for the LW scheme, the similar deviations are observed for the initial bump profile, see Fig.13. Therefore, among the terms appearing in the differential approximation of these scheme, the fourth order dissipation term is, as expected, the most influential for the shape of the travelling wave.

This third-order scheme also demonstrates an agreement with the asymptotic solution (5), (7), (10) in the dependence of the amplitudes of overshoots and undershoots with an increase in the temporal step. According to Eq. (21) δq decreases as the temporal step increases. Numerical results have shown periodic oscillations of both the overshoot and overshoot. Fig. 14 reports the range of variation of these oscillations. However, Fig. 14 shows that the undershoot always decreases as the time step increases whereas the largest value of the overshoot keeps stable.

3.3 Suppression of perturbations by artificial nonlinear terms

Finally, let us try to add artificial cubic non-linear term in the LW scheme to achieve smooth profile as shown at the end of the previous section, see Eq.(13). In this case the LW scheme has been modified by adding it using the following discretisation scheme,

$$\nu_{NL}\;\frac{(u_{j+1}^n)^3 - 2(u_j^n)^3 + (u_{j+1}^n)^3}{\triangle x^2},$$

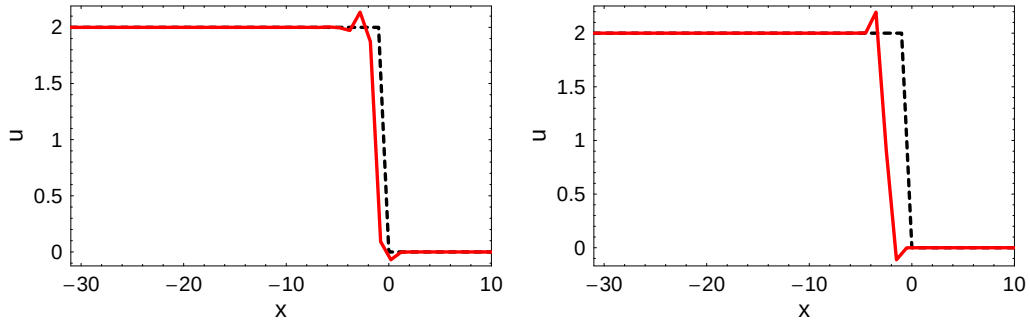

Figure 12: Propagation of an initial abrupt front using the LW3 scheme with artificial viscosity at time t = 500 (i.e. the front has propagated along 500 mesh sizes). a) $\triangle t = 0.2$; b)$\triangle t = 0.5$

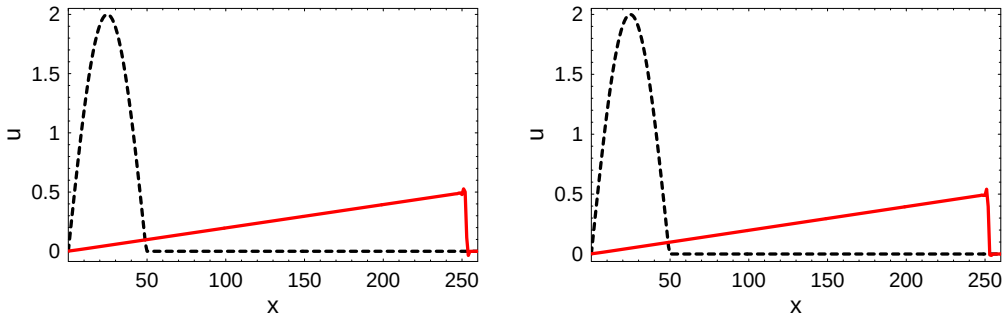

Figure 13: Propagation of an initial localized pulse using the LW3 scheme with artificial viscosity at time t = 500 (i.e. the front has propagated along 500 mesh sizes). a) $\triangle t = 0.2$; b)$\triangle t = 0.5$

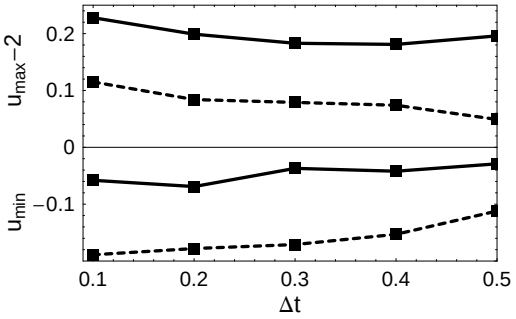

Figure 14: Variations of minimum and maximum of the shock vs temporal step for the LW3 scheme: both u_{max}-2 and u_{min} vary between upper(lower) solid and upper(lower) dotted lines.

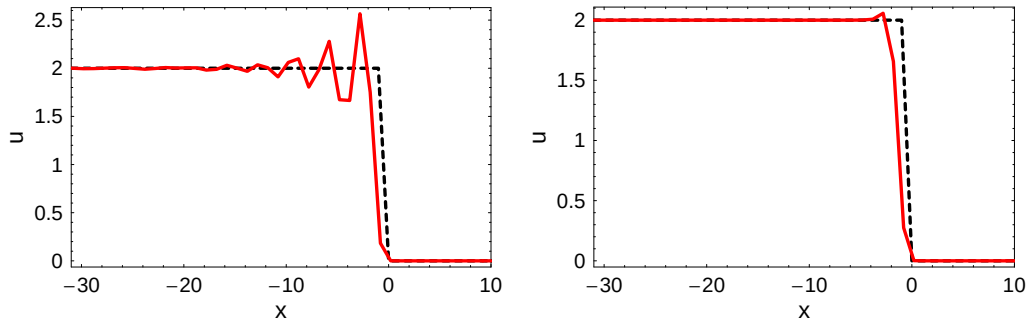

Figure 15: Improvement of the LW scheme by adding artificial non-linear cubic term at $\triangle t = 0.2$. a) $\nu_{NL} = -0.01$; b)$\nu_{NL} = 0.05$

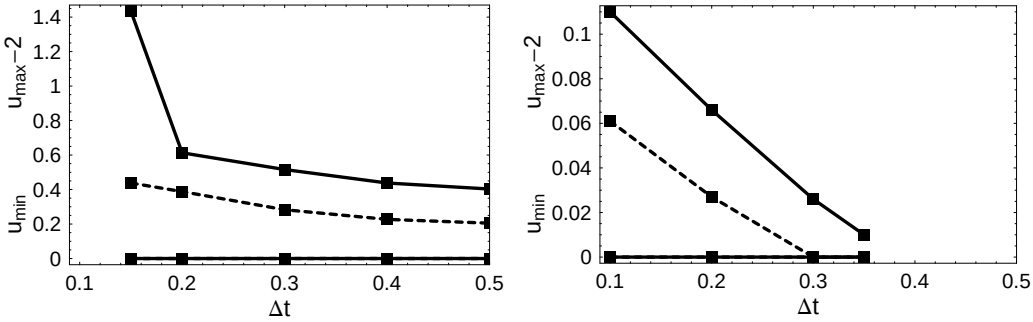

Figure 16: Variations of maximum between upper solid and dotted lines for a) $\nu_{NL} = -0.01$; b)$\nu_{NL} = 0.05$

that yields the differential approximation Eq.(13) with $\nu_{NL} = -\delta\,\alpha$. It is found that, indeed, stronger perturbations take place for negative value of ν_{NL}, c.f. Fig. 4(a) and 15(a), while a smoothness of the profile is achieved for positive ν_{NL}, c.f. Figs. 4(b) and 15(b).

Figure 16 illustrates deviations in the maximum vs temporal step. One can see in Fig. 16(b) that increase in the step provides vanishing of the overshoot.

4 Conclusions

The main result of the paper is that particular asymptotic solutions of the differential approximation of a numerical scheme for the Burgers' equation predict shock profiles arising in numerical study of a nonlinear partial differential equation. The solutions provide us with the explicit relationships between the parameters of the scheme and the coefficients in the equation responsible for dispersion or higher-order dissipation. It allows us to choose these parameters so as to avoid one or another perturbation of the numerical shock profile as demonstrated in the last section. Thus, for second order schemes our analysis shows that positive dispersion term generates overshoot at the shock profile, negative dispersion term gives undershoot at the shock profile,

this is confirmed by numerical simulations with LW and BW schemes. If dispersion coefficient vanishes (Mac-Cormack scheme with special choice of time step), the profile is almost unperturbed. For the third order scheme our analysis shows that fourth order dissipation generates symmetric overshoots and undershoots. We are able to predict deviations in the shock in dependence of the value of the steps of a numerical scheme. Therefore, the scheme deviations of the numerical shock may be diminished by choosing suitable values according to our asymptotic analysis. Also we manage to compensate the influence of dispersion by adding artificial nonlinear term. It is asymptotic solution that helps us to choose suitable term to avoid unreasonable perturbations on the shock profile.

The non-linear advection equation is chosen to demonstrate the efficiency of our approach excluding huge analytical solutions. The asymptotic travelling wave solutions of the differential approximation predict steady deviations, such as "hats", in the profile of the Burgers shock wave which are confirmed numerically. This happens even outside the formal applicability of the asymptotic solution when the parameter of the expansion δ is not small, $\delta = O(1)$.

A more rigorous mathematical justification of the method is improbable since the differential approximations belong to the class of so-called non-integrable equations. However, the method is not restricted to rather simple advection equation. The applicability of the method to more complicated equations, e.g., gas-dynamics equations will be the topic of future work.

Acknowledgment

This work of one of the authors (AVP) was supported by CEA/DAM grants 0401S/DIR and 0611S/DIR. Another author, G.B., is grateful to Dr.Antoine Llor for valuable discussion and assistance regarding use of Mathematica software and full understanding of its intricacies.

5 Bibliography

[Sh 83] Shokin Yu., (1983), "The Method of Differential Approximation", Springer, Berlin.
[BBR 03] Bouche D., Bonnaud G., and Ramos D., (2003), "Comparison of numerical schemes for solving the advection equation". Appl. Math. Lett., **16** 147–154.
[MPP 83] Mukhin S.I., Popov S.B., and Popov Yu. P., (1983), "On difference schemes with artificial dispersion", Numerical Math. and Math. Phys. **6**, 45–53.
[LP 75] Lerat A. and Peyret R., (1975), "Propriétés dispersives et dissipatives d'une classe de schémas aux différences pour les systèmes hyperboliques non linéaires", La Recherche Aérospatiale, No2, 61–79.
[E 99] Engelberg S., (1999), "An analytical proof of the linear stability of the viscous shock profile of Burgers' equation with a fourth order viscosity", SIAM J. Math. Anal., **30** 927–936.
[AS 81] Ablowitz M. and Segur H., (1981), "Solitons and inverse scattering transform", SIAM, Philadelphia.

[W 74] Whitham G.B., (1974), "Linear and Nonlinear Waves", Wiley, New York.
[F 91] Fletcher C.A.J., (1991), "Computational Techniques for Fluid Dynamics 2. Specific Techniques for different flow categories", Springer, Berlin.